JOURNAL OF MAGNETIC RESONANCE **135,** 30–36 (1998)
ARTICLE NO. MN981540

In Vivo Multiple Spin Echoes

A. Bifone,[1] G. S. Payne, and M. O. Leach

CRC Clinical Magnetic Resonance Research Group, The Institute of Cancer Research, and The Royal Marsden NHS Trust, Sutton, Surrey SM2 5PT, United Kingdom

E-mail: bifone@icr.ac.uk

Received February 11, 1998; revised June 9, 1998

The demagnetizing field produced by the nuclear polarization can induce refocusing of multiple spin echoes. We show that multiple spin echoes can be observed *in vivo* **with a clinical MR system at 1.5 T. Strategies for the spatial localization of the multiple spin echo signals are considered. Multiple spin echo studies in brain white matter and skeletal muscle in healthy volunteers are reported. The dependence of the signal amplitudes on the experimental parameters is compared with the theory. The sources of contrast for MRI and the perspectives for medical applications are discussed.** © 1998 Academic Press

Key Words: **multiple spin echoes; diffusion;** *in vivo;* **demagnetizing field; localization.**

I. INTRODUCTION

The effect of the small contribution of the nuclear polarization to the bulk susceptibility is normally neglected in NMR experiments. In highly polarized systems and in concentrated solutions, however, the nuclear dipolar demagnetizing field can have important consequences. In particular, when the longitudinal magnetization of the spin system is spatially modulated, the nuclear dipolar field significantly perturbs the evolution of the transverse component of the magnetization. A conceptually simple case is the refocusing of *m*ultiple spin *e*choes (MSEs) following the two RF-pulse sequence of Fig. 1. In the evolution period between the two pulses, the transverse magnetization is dephased by the applied field gradient and forms a helix structure in the rotating frame. The final pulse results in a sinusoidal modulation of the longitudinal and transverse components of the magnetization. Although a single echo is predicted by the solution of the Bloch equations, multiple spin echoes at times 2τ, 3τ, etc., have been observed in solid (*1*) and liquid (*2, 3*) He and, more recently, in water (*3, 4*). This phenomenon has been explained by including the effect of the demagnetizing field in the Bloch equations (*1–3*), which, in the presence of a strong linear field gradient along **z,** can be written

$$\frac{d\mathbf{M}}{dt} = \gamma[\mathbf{M} \times (B_0 + G_z s + \mu_0 M_z)\hat{\mathbf{z}}] - \frac{(M_z - M_0)\hat{\mathbf{z}}}{T_1} - \frac{(M_x\hat{\mathbf{x}} + M_y\hat{\mathbf{y}})}{T_2} + D\frac{d^2\mathbf{M}}{dz^2}. \quad [1]$$

The additional term introduced by the nuclear demagnetizing field makes the equation non-linear in the magnetization M. The solution of these non-linear Bloch equations can be expressed as a superposition of harmonics whose amplitudes decrease with the order of the harmonic (*3*). The *n*th-harmonic generated by the spatial modulation of the longitudinal magnetization is refocused by the field gradient at a time $n\tau$, and produces a spin echo.

Lee *et al.* (*5*) have shown the connection between the demagnetizing field and intermolecular dipolar couplings. Molecular tumbling effectively decouples spins that are separated by much less than the molecular diffusion distance on the time scale of the NMR experiment. The residual dipolar couplings between distant spins are responsible for the dipolar demagnetizing field, and can give rise to intermolecular multiple quantum coherences (*6*). The sensitivity of intermolecular Zero Quantum Coherences to susceptibility variations in rat brain has been recently demonstrated by Warren and co-workers (*7*). In a uniform spherical sample the net dipolar field is zero, because of the symmetry of the dipolar interaction. When a modulation of the longitudinal magnetization is introduced, *e.g.,* by the sequence of Fig. 1, the symmetry is broken, and the spins experience a net dipolar field. The dipolar nature of the demagnetizing field is apparent in the dependence of the amplitude of the multiple spin echoes on the direction of the applied field gradients. When the modulation of the longitudinal magnetization is along an axis at an angle of 54.7° degrees with respect to the static magnetic field (the "magic angle"), the effect of the demagnetizing field vanishes, and no multiple spin echoes are observed.

The potential application of multiple spin echoes in MRI and in *in vivo* NMR has been envisaged by several authors (*8–10*), mainly in relation to diffusion studies. The modulation of the

[1] To whom correspondence should be addressed.

1090-7807/98 $25.00

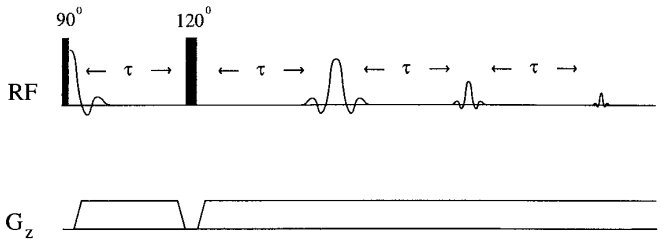

FIG. 1. A simple pulse sequence used to generate multiple spin echoes.

longitudinal magnetization is destroyed by diffusion processes, causing the dipolar demagnetizing field to vanish for long echo times. Thus the second echo amplitude strongly depends on the apparent diffusion coefficient of the spins, and multiple spin-echo imaging might represent an alternative to *p*ulsed *g*radient *s*pin *e*cho (PGSE) studies. Multiple spin echo experiments can also be used to probe the structure of heterogeneous samples (*11*). In fact, the echo amplitude is sensitive to sample structure on a length scale equal to the pitch of the spatially modulated longitudinal magnetization (*9, 11*). Intereference phenomena have been predicted for samples with periodic structures (*11*). Thus, in spite of the intrinsic low sensitivity, MSEs are potentially very interesting for *in vivo* characterization of tissues and for MRI.

Multiple spin echoes have previously been observed in very high magnetic fields. In this paper, we show that MSEs can be detected *in vivo* at relatively low magnetic fields, such as those used in clinical MRI. Sequences for spatially localized MSE experiments have been developed to study MSEs *in vivo* in specific tissues. We have investigated the dependence of the MSE amplitudes on experimental parameters in skeletal muscle and in brain white matter in healthy volunteers. The sources of contrast in MSE imaging are discussed. We show that finite T_2 effects are important, especially in skeletal muscle. The dependences of the MSE amplitudes on gradient strength and echo time in tissues and in homogeneous samples are compared. Whereas MSEs in homogeneous samples can be described by a simple theory, the heterogeneity of tissues makes the interpretation of the data less straightforward. The perspectives for medical applications of MSE imaging are discussed.

II. MSEs WITH A CLINICAL MRI SCANNER

The amplitudes of the multiple spin echoes depend on the magnetization of the spin system, and are larger for larger magnetic fields. Second spin echo amplitudes of the order of a few percent of the first echo have been observed in water (*3*) at 11.7 T. However, the amplitudes of the multiple spin echoes also depend on the strength of the applied field gradient G. The solution of Eq. [1] neglecting T_1 effects predicts a ratio of the second to first echo amplitude (*15*),

$$\frac{a_2}{a_1} = e^{2D^*/3}\beta F(D^*)e^{-2\tau/T_2}, \qquad [2]$$

where

$$\beta = \mu_0\gamma\Delta M_0[D(\gamma G)^2]^{-1/3} \qquad [3]$$

and

$$F = \frac{1}{2}\pi^{1/2}D^{*-1/6}e^{-7D^*/3}\mathrm{erf}(D^{*1/2}). \qquad [4]$$

D^* is a function of τ, of the diffusion constant D and of the applied field gradient G,

$$D^* = (\gamma^2G^2)D\tau^3 \qquad [5]$$

and $\Delta = \frac{1}{2}(3\cos(\theta)^2 - 1)$, where θ is the angle between the gradient and **z.** The amplitude of the second echo is maximum for a gradient parallel to ***z***, and vanishes when $\theta = 54.7°$ degrees.

It is apparent from Eqs. [2]–[4] that, for a given D*, larger gradients result in smaller multiple echoes. The minimum strength of the gradient is limited by the size of the sample. Indeed, in order to have a sinusoidally modulated longitudinal magnetization, the variation of the magnetic field through the sample has to be much larger than the demagnetizing field (*3*). For large samples, multiple spin-echoes can be observed at relatively low magnetic fields, such as those used in routine clinical MRI.

Figure 2 shows ^{1}H echoes obtained with the sequence of Fig. 1 at 1.5 T in a clinical Siemens Vision scanner. The sample consisted of a 18-cm-diameter Perspex sphere filled with deionized water (resistivity $>$ 18 MΩcm). The signal was acquired with a circularly polarized ^{1}H head coil. A gradient of 1 mT/m was applied along the direction of B_0, and the interpulse interval τ was set to 50 ms.

Figure 3 shows the dependence of ratio of the second to the first echo amplitude on the strength of the applied field gradient

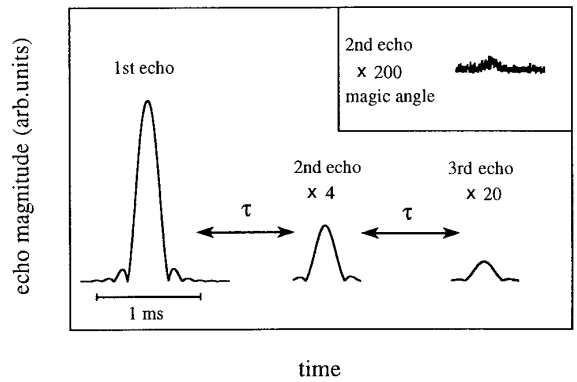

FIG. 2. Measured 1st, 2nd, and 3rd echoes in water at 1.5 T with $\tau = 50$ ms and a gradient of 1 mT/m along *z*. Inset: 2nd echo measured when gradient is at magic angle to B_0.

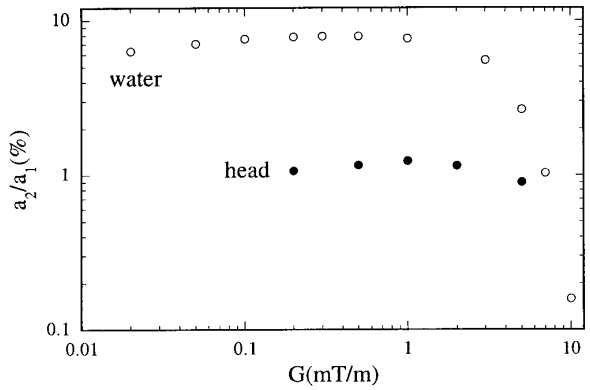

FIG. 3. Ratio of the 2nd to the 1st echoes acquired with the sequence of Fig. 1 from a water phantom and from the head of a volunteer as a function of the strength of the gradient applied along z (τ = 50 ms).

in the water phantom and in the head of a volunteer. In water, values close to 8% were observed for gradients below 1 mT/m. The amplitudes of the MSEs in tissues are smaller, and present a different dependence on the applied field gradients. In order to study the dependence of the *in vivo* MSEs on the experimental parameters and to discriminate between different tissues, it is necessary to develop a technique for the spatial localization of MSEs. Some of the possible strategies are discussed in the next section.

III. SPATIALLY LOCALIZING MSEs

The simplest way to acquire MSEs from a selected volume is to combine the basic sequence of Fig. 1 with a standard volume-selective spectroscopy sequence. We have studied three different schemes, based on some of the most popular localization sequences, ISIS (*12*), PRESS (*13*), and STEAM (*14*). The three sequences are shown in Figs. 4a–4c, respectively.

ISIS relies on the cancellation of the signal contribution from regions out of the volume of interest by applying combinations of three selective inversion pulses which define a cuboid of material. We found that, although this approach yields an efficient localization of the first echo, it is not effective for the second echo. The reasons are apparent in Fig. 5, which shows two subscans of the sequence of Fig. 4a, one involving just a read pulse, and one preceded by a single

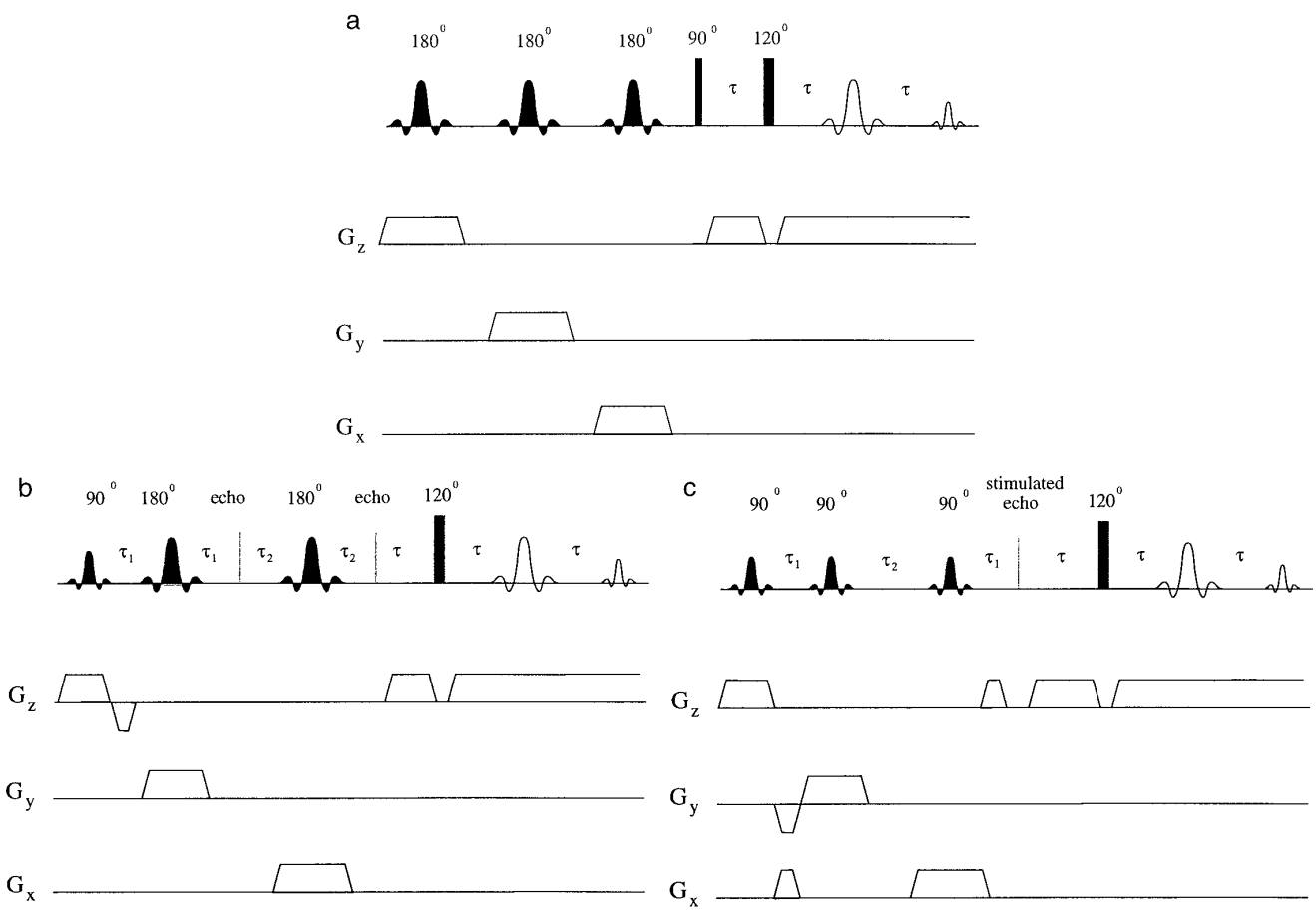

FIG. 4. Possible sequences to acquire multiple spin echoes from a localized volume. (a) ISIS-MSE, (b) PRESS-MSE, and (c) STEAM-MSE.

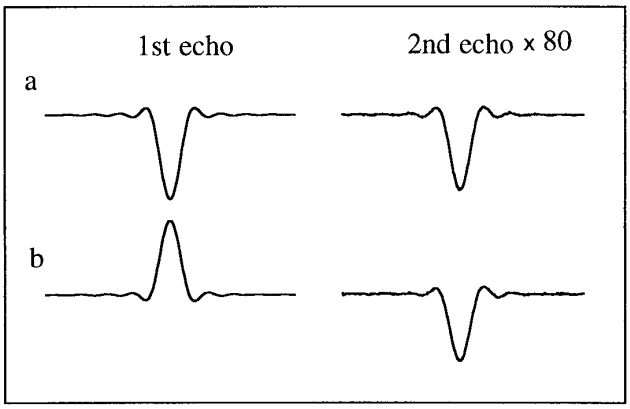

FIG. 5. The 1st and 2nd echoes for ISIS-MSE subscans. (a) 90°–120°–acq. (b) 180°–90°–120°-acq.

inversion pulse. Whereas the phase of the first spin echo is reversed by the initial inversion pulse, the phase of the second echo is not. In fact, the initial inversion pulse results in a phase inversion of the spatial modulation of the longitudinal magnetization, and a consequent 180° degrees shift of the second echo phase, which compensates the effect of the inversion pulse. Thus, when the 8 experiments corresponding to the combinations of the three initial inversion pulses are added together, the second spin echo from the volume of interest is cancelled to the same extent as the contribution from the external region, and no signal is observed. In conclusion, localization schemes based on selective inversion of the magnetization in the volume of interest are not straightforwardly applicable to MSEs.

More promising are single-shot approaches where the region of interest is selectively excited, such as PRESS (Fig. 4b) or STEAM (Fig. 4c). In PRESS, a selective 90° pulse is applied to a slice, and the signal is refocused by two selective 180° pulses applied to orthogonal slices. Only the signal from the volume of interest is refocused after the third pulse. At this point, we have applied the field gradient that spatially modulates the magnetization, and the final 120° pulse to refocus the multiple echoes.

The PRESS-MSE sequence has been applied to a test object designed to estimate the accuracy of localization techniques (*16*). The sample consists of a 15-cm-diameter sphere filled with an aqueous solution containing 0.1 m*M* GdDTPA, 0.05 m*M* $MnCl_2$, and 90 m*M* NaCl, to obtain typical coil loading conditions. The longitudinal and transverse relaxation times were 800 ms and 200 ms, respectively. A 5-cm Perspex cube filled with polydimethylsiloxane ($T_1 = 785$ ms, $T_2 = 195$ ms) was suspended in the aqueous solution. The ratio of the amplitudes of the second to the first echo for $(4\text{ cm})^3$ volumes selected in each material and as a function of τ is shown in Fig. 6. The maximum relative amplitude of the second spin echo observed in oil is smaller than in water, due to the different proton concentrations in the two liquids (approximately 70 *M* in the oil and 110 *M* in water). The dependence of the second to first echo amplitude on the evolution time τ is also different, due to the different self-diffusion coefficients in water and in oil. Whereas the diffusion of water molecules results in a consistent attenuation of the modulation of the magnetization for the longer values of τ, the high viscosity of the polydimethylsiloxane ensures appreciable MSEs in the entire range of τ explored. The lines in Fig. 6 show the result of fitting the experimental data with Eq. [2]. For water, we have used the experimental T_2 and a diffusion coefficient of 2.5×10^{-5} cm^2 s^{-1}, the only fitting parameter being a scaling prefactor. The agreement between the data and the theory is very good. For the oil, the prefactor has been fixed by rescaling the prefactor for water by the different concentration of protons, and the diffusion coefficient has been used as a fitting parameter. The fitting procedure yields $D = 0.38 \times 10^{-5}$ cm^2 s^{-1}.

The relative amplitude of the second echo obtained with the PRESS-MSE is smaller than that obtained with the unlocalized MSE sequence on the same sample. This attenuation is caused by T_2 relaxation during the first part of the localizing sequence. The smaller amplitude of the spatially modulated longitudinal magnetization after the last pulse results in a net reduction of the MSE amplitude. In STEAM, the magnetization is stored along the *z* axis by the second 90° pulse and is recalled using a third 90° pulse. This sequence produces stimulated echoes with a net loss of a factor 2 in the magnitude of the refocused magnetization. The amplitudes of the MSEs generated by the following 120° pulse are further reduced due to the smaller longitudinally modulated magnetization. Thus, STEAM-MSE is in principle less efficient than PRESS-MSE. However, STEAM-MSE might be advantageous in the case of very short T_2, when the transverse relaxation during the localization part of PRESS-MSE would result in a dramatic loss of signal.

We have observed occasional refocusing of spurious echoes following the PRESS-MSE sequence. These echoes are likely to be due to pulse imperfections, which cause antiphase mag-

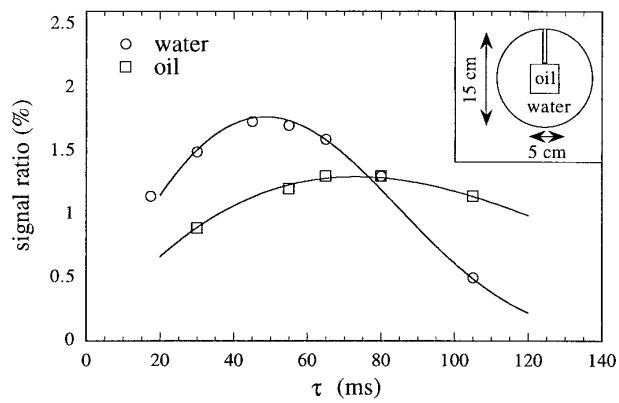

FIG. 6. Ratio of the 2nd to the 1st echo amplitude for water and polydimethylsiloxane as a function of τ for $G_z = 1$ mT/m. The solid lines are fits to Eq. [2]. Inset: Schematic of the test object designed to test the accuracy of localization techniques.

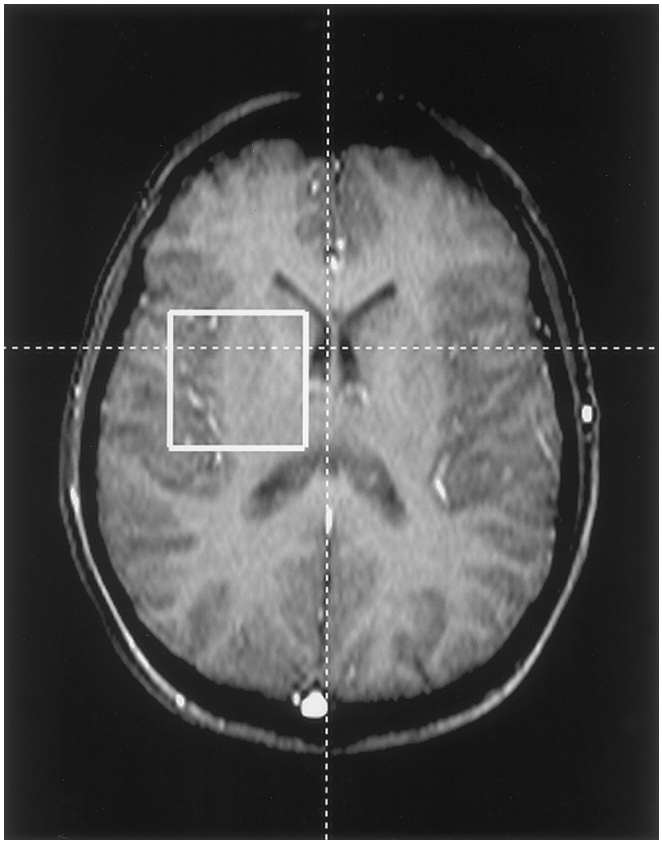

FIG. 7. Transverse 2D FLASH MR image of a volunteer's brain. The white box indicates the $4 \times 4 \times 4$ cm^3 voxel chosen for the MSE measurement.

netization terms at the end of the localizing part of the sequence. These antiphase terms are then refocused under the effect of the field gradient after the last pulse. Even small pulse imperfections can cause echoes of amplitude comparable to that of the multiple spin-echoes, since they come from extended regions of the sample. Control experiments with the gradient set at the magic angle with respect to the static magnetic field have been performed to discriminate MSEs from these undesirable echoes.

IV. *IN VIVO* MEASUREMENTS: RESULTS AND DISCUSSION

We have acquired MSEs from calf muscle and brain white matter in healthy volunteers. The sensitivity attainable at 1.5 T allowed detection of the first and second echoes only. For the brain studies, we have used PRESS-MSE to localize a volume of interest of (4 cm)^3 (Fig. 7). Even if a contribution from grey matter is expected from such a large volume, the signal intensity should be dominated by white matter. The data were acquired with a circularly polarized Siemens head coil. In Fig. 8 we show the dependence of the ratio of the second to first echo amplitudes on the echo time for two values of the applied

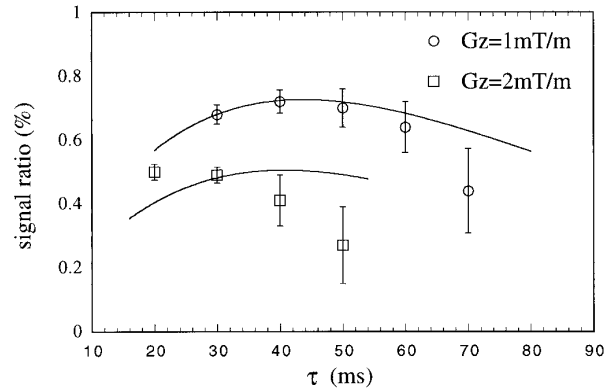

FIG. 8. Ratios of 2nd to 1st MSE signals from the brain of a volunteer (localized volume shown in Fig. 7) as a function of τ for two different gradient strengths. The solid lines have been generated by fitting Eq. [2] to the experimental data.

field gradient. The gradient was aligned along the magnetic field (z direction). A long repetition time ($TR = 8$ s) was used to avoid interscan stimulated echoes. Figure 9 shows the experimental MSEs from the calf of a volunteer. The signal was acquired with the basic unlocalized MSE sequence of Fig. 1. The volunteer was lying supine, with the calf muscle fibres approximately aligned with the B_0 magnetic field. A circularly polarized Siemens "extremity" coil was used for this experiment. Data were acquired both with the gradient along B_0 (and hence parallel to the muscle fibers) and with the gradient orthogonal to the B_0 field.

Equation [2] provides an insight into the dependence of the signal ratio upon the NMR parameters. If diffusion and T_2 relaxation are neglected, the signal intensity increases with increasing echo time and asymptotically reaches an equilibrium value determined by the magnetization M_0. However,

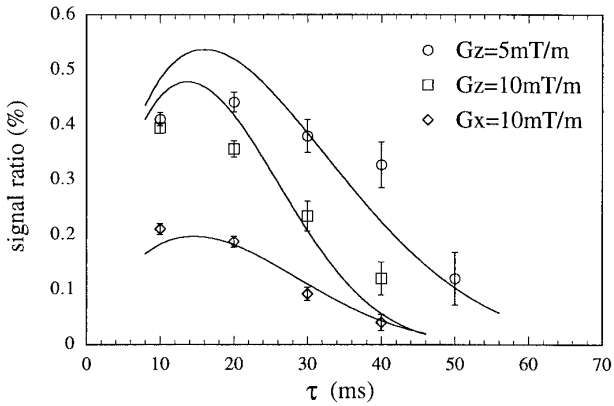

FIG. 9. Ratios of the 2nd to the 1st echoes from the calf of a volunteer acquired with the basic sequence of Fig. 1 as a function of τ and of gradient strength and orientation. The solid lines are fits to Eq. [2]. The phase of the 2nd echoes acquired with the gradient orthogonal to the static magnetic field B_0 is inverted with respect to the phase of the 2nd echoes acquired with the gradient along B_0, as expected from Eqs. [2]–[5].

molecular diffusion blurs the modulation imposed on the longitudinal magnetization, and results in a decay of the signal ratio for long echo times. Similarly, T_2 relaxation mechanisms cause the signal ratio to decay with increasing echo times. The second echo amplitude is affected by diffusion and T_2 processes more strongly than the first echo. In addition to the obvious increase in contrast due to the extra evolution time τ, the second echo amplitude depends on the amplitude of the spatially modulated longitudinal magnetization, which is affected by decay processes during the first evolution period. Thus, the second echo decay is determined by a factor $\exp(-4\tau/T_2)$. In principle, MR imaging with MSEs offers better diffusion and T_2 contrast than conventional spin-echo techniques, at the cost of much reduced sensitivity.

Equation [2] gives a good description of the experimental data for homogeneous systems, such as the water and oil phantoms described in the previous section. In tissues, however, the agreement between the theory and the experiments is much poorer. In Figures 8 and 9, we report the result of the fit of Eq. [2] to the *in vivo* experimental data. We have used $T_2 =$ 90 ms and $T_2 = 35$ ms for white matter and skeletal muscle, respectively (*17*). In white matter, PGSE measurements (*18*) yield apparent diffusion coefficients in the range $0.4–1.3 \times 10^{-5}$ cm^2 s^{-1} dependent on the orientation of the field gradient with respect to the myelin fibers. In our fit, we have used the average of the diffusion coefficient in the different orientations, since the myelin fibers do not present homogeneous orientation in the large volume investigated.

Skeletal muscles also present anisotropic apparent diffusion coefficients of 2×10^{-5} cm^2 s^{-1} and 1.1×10^{-5} cm^2 s^{-1}, parallel and perpendicular to the fibers, respectively. For the calf, we have used these two values for the the two orientations of the gradient (z and x, respectively) (*18*).

The discrepancy between theory and *in vivo* data is not surprising. In fact, Eq. [2] is obtained by solving the modified Bloch equations (Eq. [1]) for an homogeneous system, while tissues are highly heterogeneous. The amplitude of the MSEs is sensitive to the tissue structure via several parameters.

The diffusion coefficient of Eq. [1] is a constant only in the case of homogeneous systems. In tissues, the measured apparent diffusion coefficient depends on the length of the diffusion path probed by the experiment (i.e., for a certain value of the gradient, on the echo time and restricted diffusion boundaries). In fact, water diffusion in biological tissues is hindered by the presence of cell membranes, organelles, and supracellular structures. For short paths, the probability of a molecule encountering a barrier is smaller than for long paths. For multiple spin echoes, the relevant diffusion path length is related to the pitch of the modulation of the magnetization:

$$P = 2\pi(\gamma G\tau)^{-1}. \qquad [6]$$

By varying the pitch, it should be possible to weight the MSE image by the apparent diffusion coefficients characteristic of different diffusion lengths.

Another effect of the sample heterogeneity has been elegantly demonstrated in Ref. (*11*). Warren *et al.* (*8*) first noted that in the presence of a spatially modulated magnetization, the dipolar field experienced by a specific spin results mainly from the magnetization within a distance shorter than the pitch of the modulation. When the wavelength of the modulation is comparable to the characteristic length scale of the structure of the sample, the signal ratio depends on the local magnetization, rather than on the average magnetization. This allows the sample structure to be probed at a length scale that is related to the pitch of the modulation. This new source of contrast is potentially very important for tissue characterization, since it provides information on the microscopic structure of the tissue without requiring high spatial resolution. Tissues present structures at several length scales, from a subcellular level to macroscopic supracellular structures, and the heterogeneity is expected to affect the signal ratio in a wide range of τ. An opportune choice of τ and of the gradient strength should allow probing the tissue at specific lengthscales. A theoretical approach to MSEs in heterogeneous systems is presented in Refs. (*9, 11*). However, the current theory only applies to the case of non-restricted diffusion, and further developments are necessary to interpret MSEs in tissues.

It is apparent from the fit reported in Fig. 8 that the basic theory of Eq. [2] underestimates the decay of the second echo amplitude with τ. With increasing τ, *i.e.*, for a shorter pitch of the spatially modulated longitudinal magnetization, the experiment probes shorter diffusion lengths. For short diffusion lengths, the water molecules are less likely to encounter boundaries, and the apparent diffusion coefficient is larger. This might cause the faster decay of the MSE signal observed for long τs. In our set of experiments, the pitch of the modulated magnetization ranges between 1.17 mm and 0.167 mm, which is still large when compared with the size of the fibers. It would be interesting to extend this study to shorter pitches, to increase the resolution and probe the tissue at shorter length-scales. The limiting factor is the sensitivity, which should be better at higher B_0 fields. Large deviations from the function of Eq. [2] are also observed in the calf. In that set of experiments, the shortest pitch was 0.0585 mm.

For comparison, we have also acquired first and second echoes in a gel sample (5% gelatine by weight in distilled water, $T_2 = 750$ ms). The ratio of the second to first echo amplitude is shown in Fig. 10 as a function of τ for two different gradient strengths. In this case, Eq. [2] accurately describes the dependence of the signal ratio on the experimental parameters. The fit reported in Fig. 10 gives a diffusion coefficient $D = 2 \times 10^{-5}$ cm^2 s^{-1}. Thus, tissues present a higher degree of complexity, and gels do not seem to be a good model for the tissue heterogeneity.

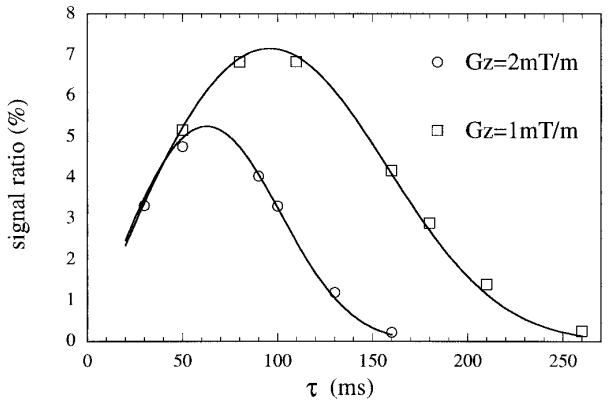

FIG. 10. Ratios of the 2nd to the 1st echoes in a gel phantom. The solid lines are fits to Eq. [2].

V. CONCLUSION

In conclusion, we have reported the first *in vivo* observation of multiple spin echoes in volunteers. The experiments were performed with a clincal MRI scanner at 1.5 T. We have developed strategies to localize the multiple spin echo signal in the volume of interest. We have studied the dependence of the second echo amplitude on echo time and on gradient strength and orientation in brain white matter and in skeletal muscle. For comparison, MSEs have been acquired in phantoms containing water, oil, and gel. The results in homogeneous samples can be interpreted with a simple theory. In tissues, large deviations from the theory are observed. Such discrepancies might arise from the heterogeneous structures of tissues. The tissue structure restricts water diffusion, and results in an apparent diffusion coefficient that depends on the pitch of the modulation imposed on the magnetization. Moreover, the modulation of the magnetization can interact with the tissue structure, and affect MSE amplitudes when the pitch is comparable to the structure lengthscale. This is a potentially very important source of contrast, which provides information on the tissue microscopic structure without requiring microscopic spatial resolution. Thus, in spite of the dramatically reduced sensitivity, MSEs might be valuable in medical MRI. The problem of sensitivity could be mitigated by increasing the field strength.

ACKNOWLEDGMENT

This work was supported by the Cancer Research Campaign [CRC] (Grant SP1780).

REFERENCES

1. G. Deville, M. Bernier, and J. M. Delrieux, *Phys. Rev. B* **19,** 5666 (1979).
2. D. Einzel, G. Eska, Y. Hirayoshi, T. Kopp, and P. Wolfle, *Phys. Rev. Lett.* **53,** 2312 (1984).
3. R. Bowtell, R. M. Bowley, and P. Glover, *J. Magn. Reson.* **88,** 643 (1990).
4. H. Körber, E. Dormann, and G. Eska, *J. Magn. Reson.* **93,** 589 (1991).
5. S. Lee, W. Richter, S. Vathyam, and W. S. Warren, *J. Chem. Phys.* **105,** 874 (1996).
6. W. S. Warren, W. Richter, A. H. Andreotti, and B. T. Farmer II, *Science* **262,** 2005 (1993).
7. W. S. Warren, S. Ahn, M. Mescher, M. Garwood, K. Ugurbil, W. Richter, R. R. Rizi, J. Hopkins, and J. S. Leigh, *Science* **281,** 247 (1998).
8. W. Richter, S. Lee, W. S. Warren, and Q. He, *Science* **267,** 654 (1995).
9. R. Bowtell and P. Robyr, *Phys. Rev. Lett.* **76,** 4971 (1996).
10. S. Mori, R. E. Hurd, and P. C. M. van Zijl, *Magn. Reson. Med.* **37,** 336 (1997).
11. P. Robyr and R. Bowtell, *J. Chem. Phys.* **106,** 467 (1997).
12. R. J. Ordidge, A. Connelly, and J. A. B. Lohman, *J. Magn. Reson.* **66,** 283 (1986).
13. P. A. Bottomley, Selective volume method for performing localized NMR spectroscopy, U.S. Patent 4 480 228, 1984.
14. J. Frahm, K. D. Merboldt, W. Hanicke, and A. Haase, *J. Magn. Reson.* **64,** 81 (1985).
15. R. Bowtell, *J. Magn. Reson.* **100,** 1 (1992).
16. M. O. Leach, D. J. Collins, S. Keevil, I. Rowland, M. A. Smith, O. Heriksen, W. M. M. Bovée, and F. Podo, *Magn. Reson. Imaging* **13,** 131 (1995).
17. J. D. de Certaines, O. Henriksen, A. Spisni, M. Cortsen, and P. B. Ring, *Magn. Reson. Imaging* **11,** 841 (1993).
18. O. Henriksen, *in* "Encyclopedia of Nuclear Magnetic Resonance" (D. M. Grant and R. K. Harris, Eds.), Vol. 3, p. 1605, Wiley, New York (1996).